Nuclei-Induced Frequency Focusing of Electron Spin Coherence
A. Greilich *et al.*
Science **317**, 1896 (2007);
DOI: 10.1126/science.1146850

ronment (nearby hydrogen nuclei) (SOM text). For both sequences, the noise coefficients c_w do not statistically deviate from the scaling implied by uncorrelated errors (fig. S3), although, as noted above, this does not guarantee that the errors are uncorrelated.

Our method provides an efficient protocol for the characterization of noise in contexts where the target transformation is the identity operator, for example, a quantum communication channel or quantum memory. However, the protocol also provides an efficient means for characterizing the noise under the action of a nonidentity unitary transformation. One approach is to decompose the unitary transformation into a product of basic quantum gates drawn from a universal gate set, where each gate in the set acts on at most 2 qubits simultaneously. Hence, the noise map acting on all n qubits associated with any two-qubit gate can be determined by applying the above protocol to other $n-2$ qubits while applying process tomography to the two qubits in the quantum gate. Another approach is to estimate the average error per gate for a sequence of m gates, such that the composition gives the identity operator. Such a sequence can be generated by making use of the cyclic property $U^m = 1$ of any gate in a universal gate set or by choosing a sequence of $m-1$ random gates followed by an m^{th} gate chosen such that the composition gives the identity transformation.

References and Notes

1. P. W. Shor, *Phys. Rev. A* **52**, R2493 (1995).
2. A. M. Steane, *Phys. Rev. Lett.* **77**, 793 (1996).
3. P. W. Shor, *Proceedings of the Symposium on the Foundations of Computer Science,* 56 (IEEE press, Los Alamitos, California, 1996).
4. D. Aharonov, M. Ben-Or, *Proceedings of the 29th Annual ACM Symposium on the Theory of Computing,* 176 (ACM Press, New York, 1996).
5. A. Y. Kitaev, *Uspekhi Mat. Nauk.* **52**, 53 (1997).
6. E. Knill, R. Laflamme, W. Zurek, *Science* **279**, 342 (1998).
7. I. Chuang, M. Nielsen, *J. Mod. Opt.* **44**, 2455 (1997).
8. G. M. D'Ariano, P. Lo Presti, *Phys. Rev. Lett.* **86**, 4195 (2001).
9. M. Mohseni, D. Lidar, *Phys. Rev. Lett.* **97**, 170501 (2006).
10. H. Haffner *et al*., *Nature* **438**, 643 (2005).
11. D. Leibfried *et al*., *Nature* **438**, 639 (2005).
12. C. Negrevergne *et al*., *Phys. Rev. Lett.* **96**, 170501 (2006).
13. A. Childs, I. Chuang, D. Leung, *Phys. Rev. A* **64**, 012314 (2001).
14. J. Emerson, Y. Weinstein, M. Saraceno, S. Lloyd, D. Cory, *Science* **302**, 2098 (2003).
15. B. Levi, C. Lopez, J. Emerson, D. G. Cory, *Phys. Rev. A* **75**, 022314 (2007).
16. J. Emerson, R. Alicki, K. Zyczkowski, *J. Opt. B: Quantum and Semiclassical Optics* **7**, S347 (2005).
17. C. Dankert, R. Cleve, J. Emerson, E. Livine, quant-ph/0606161 (2006).
18. W. Dur, M. Hein, J. Cirac, H.-J. Briegel, *Phys. Rev. A* **72**, 052326 (2005).
19. D. G. Cory *et al*., *Fortschr. Phys.* **48**, 875 (2000).
20. C. Bennett, D. DiVincenzo, J. Smolin, W. Wootters, *Phys. Rev. A* **54**, 3824 (1996).
21. P. Aliferis, D. Gottesman, J. Preskill, *Quant. Inf. Comp* **6**, 97 (2006).
22. E. Knill, *Nature* **434**, 39 (2005).
23. R. Alicki, K. Lendi, *Quantum Dynamical Semigroups and Applications*, Lecture Notes in Physics **286**, 12 (1987).
24. E. Fortunato *et al*., *J. Chem. Phys.* **116**, 7599 (2002).
25. M. Nielson, *Phys. Lett. A* **303**, 249 (2002).
26. Materials and methods are available as supporting material on *Science* Online.
27. D. G. Cory, J. B. Miller, A. N. Garroway, *J. Magn. Reson.* **90**, 205 (1990).
28. U. Haeberlen, *Advances in Magnetic Resonance*, Ed. J. Waugh, Academic Press, New York (1976).

29. This work benefited from discussions with R. Blume-Kohout, R. Cleve, M. Ditty, D. Gottesman, E. Knill, B. Levi, and A. Nayak and was supported by the National Science and Engineering Research Council of Canada (NSERC) grants 250673 and 327778, Ontario Research Development Challenge Fund (ORDCF) grant 3232301-05, Army Research Office/Laboratory for Physical Sciences (ARO/LPS) grant W911NF-05-1-0469, and Army Research Office/Mathematics of Information Technology and Complex Systems (ARO/MITACS) grant W911NF-05-1-0298.

Supporting Online Material

www.sciencemag.org/cgi/content/full/317/5846/1893/DC1
Materials and Methods
SOM Text
Figs. S1 to S3
References

25 May 2007; accepted 29 August 2007
10.1126/science.1145699

Nuclei-Induced Frequency Focusing of Electron Spin Coherence

A. Greilich,[1]* A. Shabaev,[2,3]* D. R. Yakovlev,[1,4] Al. L. Efros,[2]† I. A. Yugova,[1,5] D. Reuter,[6] A. D. Wieck,[6] M. Bayer[1]†

The hyperfine interaction of an electron with the nuclei is considered as the primary obstacle to coherent control of the electron spin in semiconductor quantum dots. We show, however, that the nuclei in singly charged quantum dots act constructively by focusing the electron spin precession about a magnetic field into well-defined modes synchronized with a laser pulse protocol. In a dot with a synchronized electron, the light-stimulated fluctuations of the hyperfine nuclear field acting on the electron are suppressed. The information about electron spin precession is imprinted in the nuclei and thereby can be stored for tens of minutes in darkness. The frequency focusing drives an electron spin ensemble into dephasing-free subspaces with the potential to realize single frequency precession of the entire ensemble.

The possibility of encoding quantum information in the spins of quantum dot (QD) electrons has attracted considerable attention (*1*, *2*). The spatial confinement protects the spins against the primary relaxation mechanisms in bulk, all of which arise from coupling of spin and orbital momenta. However, the electron hyperfine interaction with the lattice nuclei is enhanced by confinement, leading to spin decoherence and dephasing (*3*–*10*) and thus posing severe difficulties for processing quantum information. General schemes for suppressing decoherence have been discussed already (*11*). Electron spin relaxation in QDs may be overcome by polarizing the nuclear spins (*12*, *13*), but the high degree of polarization required, close to 100% (*12*), has not been achieved yet (*14*–*16*).

We find that the hyperfine interaction, rather than being detrimental, can be used as a precision tool by demonstrating that it modifies the continuous mode spectrum of the electron spin precession in a QD ensemble into a few discrete modes. The information on this digital spectrum can be stored in the nuclear spin system for tens of minutes because of the long nuclear memory times (*17*, *18*).

In a QD ensemble, fast electron spin dephasing arises not only from nuclear field fluctuations but also from variations of the electron g factor, leading to different spin precession frequencies. The dephasing due to these unavoidable variations can be partly overcome by mode-locking (*19*), which synchronizes the precession of specific electron spin modes in the ensemble with the clocking rate of a periodic pulsed laser. Still, it leaves a substantial fraction of dephased electron spins, whose precession frequencies do not satisfy the mode locking conditions. We demonstrate that the nuclear spin polarization adjusts the electron spin precession frequency in each quantum dot such that the whole ensemble becomes locked on very few frequencies.

The experiments were done on an ensemble of self-assembled (In,Ga)As/GaAs QDs (*19*, *20*), each dot containing on average a single electron (*21*). The electron spin precession about a perpendicular magnetic field was studied by a pump-probe Faraday rotation (FR) technique with ps time resolution (*22*). Spin coherence is generated

[1]Experimentelle Physik II, Universität Dortmund, D-44221 Dortmund, Germany. [2]Naval Research Laboratory, Washington, DC 20375, USA. [3]School of Computational Sciences, George Mason University, Fairfax, VA 22030, USA. [4]A. F. Ioffe Physico-Technical Institute, 194021 St. Petersburg, Russia. [5]Institute of Physics, St. Petersburg State University, 1908504 St. Petersburg, Russia. [6]Angewandte Festkörperphysik, Ruhr-Universität Bochum, D-44780 Bochum, Germany.

*These authors contributed equally to this work.
†To whom correspondence should be addressed. E-mail: efros@dave.nrl.navy.mil; manfred.bayer@physik.uni-dortmund.de

by circularly polarized pump pulses with wave vector parallel to the structure growth axis (z axis) and detected by rotation of the linear polarization of probe pulses. The excitation laser emits pulses with 1.5-ps duration at a rate of 75.6 MHz, equivalent to a pulse separation T_R = 13.2 ns (see sketch in Fig. 1A). The excitation is resonant with the ground state charged exciton consisting of two electrons with opposite spins and a hole.

The top trace in Fig. 1A shows a FR signal of the QD ensemble, created by a single pump pulse train. The signal at positive delays shows a fast decay on a ns time scale due to dephasing of the spin coherence by the ensemble spread of precession frequencies. The modulation arises from neutral exciton contributions (*20*). The signal at negative delays is due to constructive interference of electron spin precession modes fulfilling the phase synchronization conditions (PSC): $\omega = 2\pi K/T_R$, where K is an integer (*19*).

Much more flexible tailoring of the mode-locked distribution of spins is possible through a two pump pulse protocol (*23*). Each pump pulse was split into a doublet with a delay $T_D = 1.86\ \text{ns} \approx T_R/7$ between the two pulses (Fig. 1A). The corresponding FR signal is shown by the middle trace in Fig. 1A. Excitation by such a pump doublet leads to a sequence of FR signal bursts, which appear not only at the moments of pump pulse arrival but also periodically before and after the pump doublet with a period equal to T_D. These bursts arise from constructive interference of modes satisfying the two pulse protocol PSC of $\omega = 2\pi K/T_D$ (*23*).

The FR signal pattern created by the two pulse protocol is memorized over minutes. One would expect that blocking of the second pulse in a pump doublet would destroy the periodic FR burst pattern on the μs time scale of the electron spin coherence time, T_2, in these dots (*19*). Only the FR signal around the first pump should remain over the scanned range of pump-probe delays. Recording of the middle trace in Fig. 1A had the sample illuminated for ~20 min by the pump-doublet train. Immediately after this measurement, the second pump was blocked, and a FR measurement using only the single pump train was started (bottom trace in Fig. 1A) beginning from negative delays. Contrary to the expectations, the signal shows qualitatively all features of a pump doublet protocol. A strong FR signal ("burst 0") appears around the delays where the second pump was located. Further signals, denoted burst 1 and burst 2, also appear. The system therefore remembers for minutes its previous exposure to a two pump protocol. The decay of the burst amplitude with the increasing burst number is due to the increasing time at which the corresponding signal was recorded since switching off pump 2.

We have recorded FR traces in a short delay range around burst 0 for different times after closing the second pump. In these traces (Fig. 1B), we observe a strong FR signal even after 40 min. Because no phase shift between the FR traces occurs, we can record the decay kinetics at a fixed delay of 1.857 ns (corresponding to the maximum FR signal) versus time after switching off pump 2 (blue curve in Fig. 1C). The observed dynamics can be well described by a bi-exponential dependence on elapsed time t, $a_1\exp(-t/\tau_1) + a_2\exp(-t/\tau_2)$, as shown by the red line fit to the data, from which we get a memory time τ_1 of 1 min, while τ_2 is 10.4 min. The decay, however, critically depends on the light illumination conditions. When the system is held in darkness (both pumps and probe are blocked), no relaxation occurs at all on an hour time scale. This is exemplified by the red circles in Fig. 1C, which give the FR amplitude when switching on pump 1 as well as the probe after a dark period t.

We have also examined how fast a two pump pulse train creates the periodic burst pattern in the

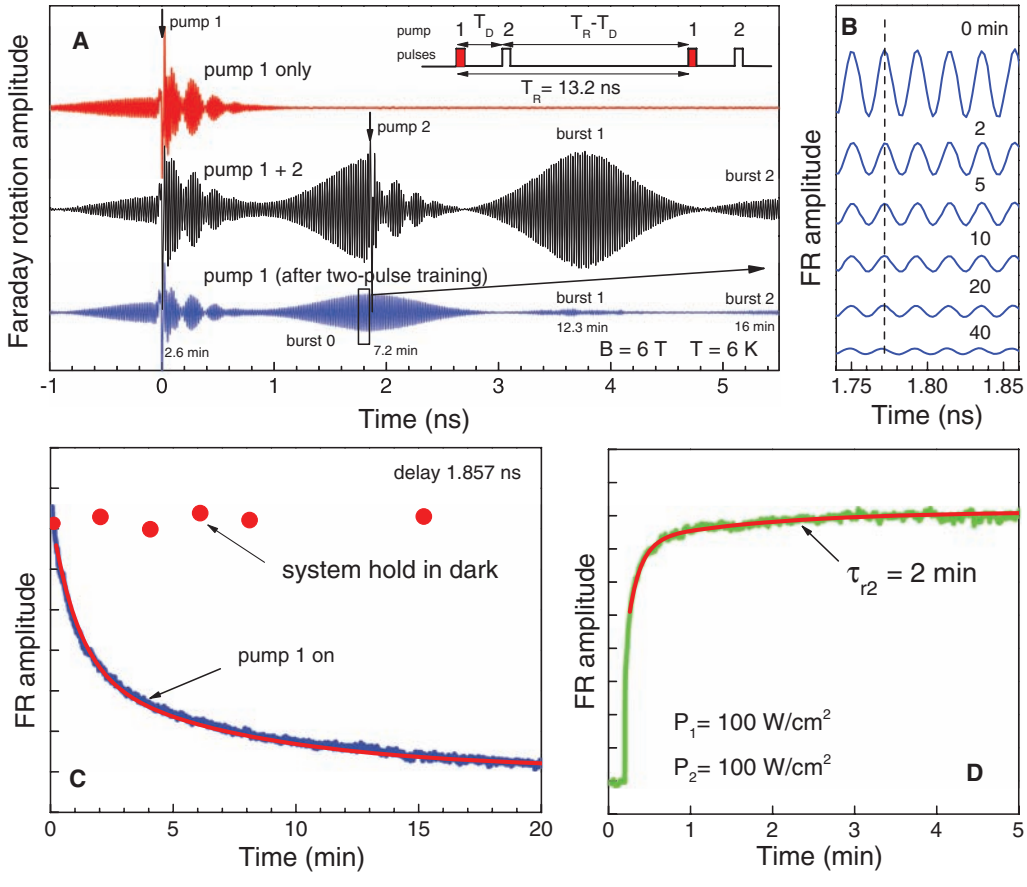

Fig. 1. (**A**) FR traces as function of delay time between probe pulse and first pump pulse measured on an ensemble of singly charged (In,Ga)As/GaAs quantum dots. The signals were scanned from negative to positive delays. Details of the optical excitation protocol are given in the sketch. The top trace was recorded for a single pump pulse train. For the middle trace we used a two pump pulse protocol with the second pump delayed by T_D = 1.86 ns relative to the first one. The lowest trace was taken for a single pump pulse. Recording started right after measurement of the middle trace. Some times at which the different FR signal bursts were measured are indicated. The pump and probe power densities were 50 and 10 W/cm^2, respectively. (**B**) FR signals measured over a small range of delay times around the burst 0 maximum [as indicated by the box in (A)] for different times after closing the second pump; at the same time, pump 1 and probe were always on. (**C**) Relaxation kinetics of the FR amplitude at a delay of 1.857 ns (maximum of burst 0) as a function of time after switching off pump 2. Beforehand, the system was treated for 20 min by the two pump pulse protocol. The blue curve was measured with pump 2 blocked at t = 0. The red line shows a bi-exponential time dependence fitted to the data. The red circles show the FR signal after keeping the system in darkness for different times and then addressing it by pump 1 and probe. (**D**) The kinetics of FR amplitude at the same delay of 1.857 ns when switching at t = 0 from the single to the two pump pulse protocol. The single pump pulse exposure before the switch lasted for 20 min. For each of the pumps the excitation density was 100 W/cm^2. The red line is a bi-exponential fit. For all panels B = 6 T and T = 6 K.

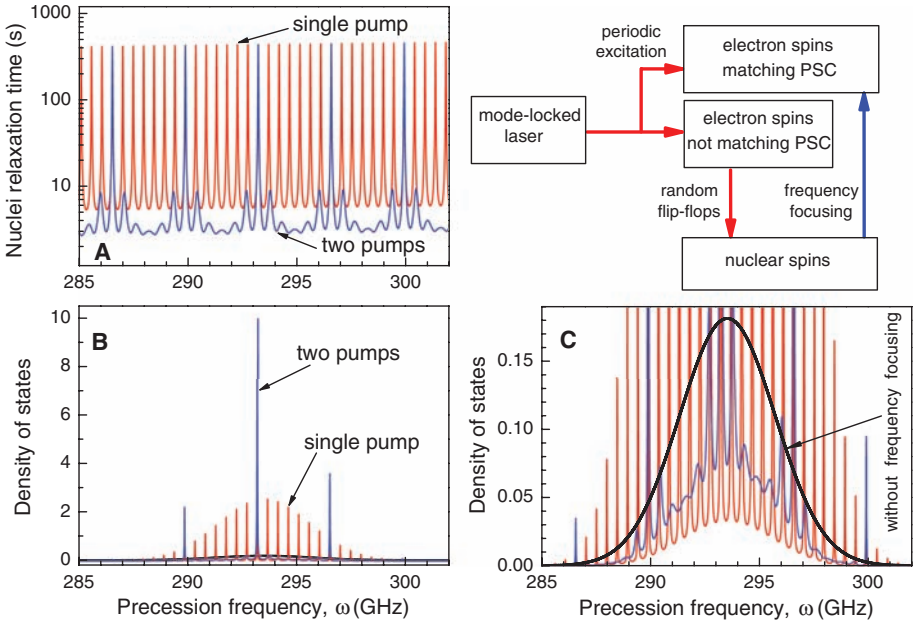

Fig. 2. Scheme of effects leading to the nuclei-induced frequency focusing of the electron spin precession modes. The periodic resonant excitation by a mode-locked circularly polarized laser synchronizes the precessions of electron spins whose frequencies satisfy the PSC. At the same time, the excitation leads to a nuclear rearrangement in those QDs, which do not satisfy the PSC, via optically stimulated electron-nuclear spin flip-flop processes. The rearrangement modifies the electron spin precession frequency such that it becomes frozen when the frequency reaches the PSC. (**A**) Average spin relaxation time of the As nuclei versus the electron spin precession frequency calculated for the single pump (red) and the two pump (blue) protocols. The spin relaxation time calculated in Eq. 11 in SOM text was derived by using (*30*, *31*). (**B**) Density of electron spin precession modes in an ensemble of singly charged QDs modified by the nuclei, calculated for the single pump (red) and the two pump (blue) protocols. The black line shows the density of modes before frequency focusing due to ensemble dispersion of electron g factor and nuclear polarization fluctuation. (**C**) A closeup of (B) for better visibility of the low density of states range. All calculations have been done for $B = 6$ T, $|g_e| = 0.555$, $\Delta g_e = 0.0037$, $\Delta\omega_{N,x} = 1$ GHz, $T_R = 13.2$ ns, $T_D = T_R/7$ ns, and $T_2 = 3$ μs.

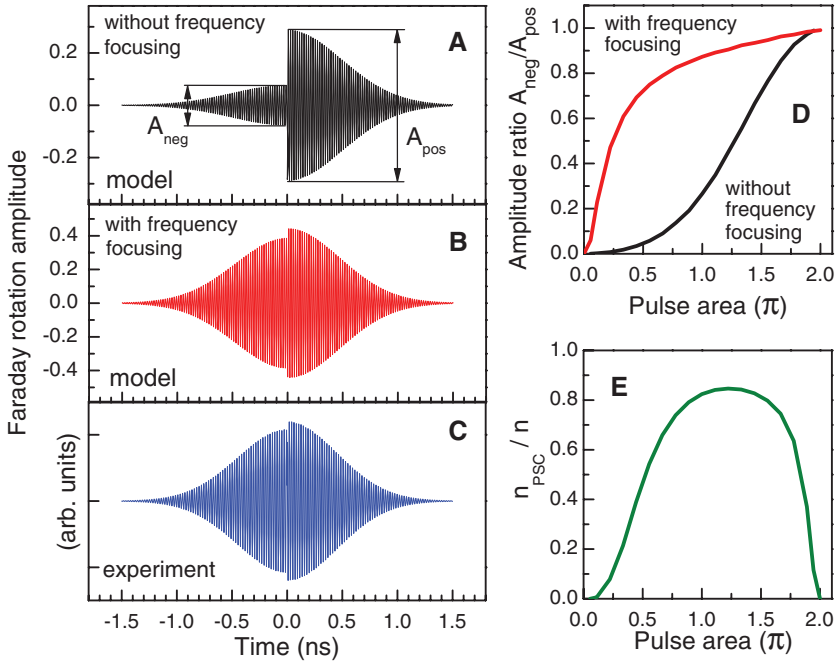

Fig. 3. (**A** to **C**) FR traces for an ensemble of singly charged QDs subject to a single pump pulse excitation protocol with pulse area $\Theta = \pi$ at $B = 6$ T. (A) FR traces calculated with the density of electron spin precession modes unchanged by the nuclei. The ratio of the FR amplitudes before, A_{neg}, and after, A_{pos}, the pump pulse shows that only 30% of the electrons are involved in the mode-locked spin precession, leading to a reduced FR signal at negative delays compared with that of positive delays. (B) FR traces calculated with the density of electron spin precession modes modified by the nuclei. The ratio of the FR amplitudes A_{neg}/A_{pos} shows that 90% of electrons are now involved in mode-locked precession. (C) Experimental trace of the FR signal obtained after extracting the contribution from neutral excitons, which leads to modulation of the FR signal after pump pulse arrival (Fig. 1). The experimental ratio A_{neg}/A_{pos} confirms that 90% of the electrons are involved in the mode-locked precession in our experiment. (**D**) Calculated ratio of the FR signal amplitudes, A_{neg}/A_{pos}, with (red) and without (black) including nuclear rearrangement as function of pump pulse area. (**E**) Dependence of the relative number of electrons, n_{psc}/n, in a QD ensemble involved in the mode-locked precession as function of pump pulse area. The same set of parameters was used as in Fig. 2.

FR signal. For that purpose, the sample was first illuminated only by pump 1, and then pump 2 was switched on. Both pumps had a power of 100 W/cm^2. The rise of the FR signal was measured at a FR maximum within burst 1 as function of time elapsed after switching on pump 2 (Fig. 1D). The slow component of this rise, τ_{r2}, is on a minutes time scale, and it shortens with excitation power.

The observed long memory of excitation protocol must be imprinted in the QD nuclei, for which long spin relaxation times in high magnetic fields up to hours or even days have been reported (*24*, *25*). The nuclei in a particular dot must have been aligned along the magnetic field, B, through the hyperfine interaction with the electron during exposure to the pump train. This alignment, in turn, changes the electron spin precession frequency, $\omega = \omega_e + \omega_{N,x}$, where $\omega_e = g_e\mu_B B/(\hbar)$, μ_B is the Bohr magneton, g_e is the electron g factor, and the nuclear contribution, $\omega_{N,x}$, is proportional to the nuclear polarization. The slow rise and decay dynamics of the FR signal in Fig. 1 indicate that the periodic optical pulse train stimulates the nuclei to increase the number of QDs for which the electron spin precession frequencies satisfy the PSC for a particular excitation protocol.

What is driving the projection of the nuclear spin polarization on the magnetic field to a value that allows an electron spin to satisfy the PSC?

The nuclear polarization is changed by electron-nuclear spin flip-flop processes resulting from Fermi-contact hyperfine interaction (*26*). Such processes, however, are suppressed in a strong magnetic field because of the energy mismatch between the electron and nuclear Zeeman splittings by about three orders of magnitude. Flip-flop transitions, which are assisted by pho-

nons compensating this mismatch, have a low probability because of the phonon bottleneck in QDs (*27*, *28*). This explains the robustness of the nuclear spin polarization in darkness to over an hour (Fig. 1C).

Consequently the resonant optical excitation of the singlet trion becomes the most efficient mechanism in the nuclear spin polarization dynamics. The excitation process rapidly turns "off" the hyperfine field of a resident electron acting on the nuclei, and the field is subsequently turned on again by the trion radiative decay. Thereby it allows a flip-flop process during the switching without energy conservation.

The nuclear spin-flip rate for this mechanism is proportional to the rate of optical excitation of the electron, $\Gamma_l(\omega)$. According to the selection rules, the probability of exciting the electron to a trion by σ^+ polarized light is proportional to $1/2 + S_z(\omega)$, where $S_z(\omega)$ is the component of the electron spin polarization along the light propagation direction taken at the moment of pump pulse arrival. Therefore, the excitation rate $\Gamma_l(\omega) \sim [1/2 + S_z(\omega)]/T_R$. For electrons satisfying the PSC (*19*): $S_z(\omega) \approx -1/2$, the excitation probability is very low because of Pauli blocking. Because of a very long decoherence time, T_2, in our QDs, the excitation rate for these electrons is reduced by two orders of magnitude to $1/T_2$ from $1/T_R + 1/T_2$ for the rest of electrons (in our experiments $T_2/T_R \approx 200$) [Supporting Online Material (SOM) text].

Because of $\Gamma_l(\omega)$, the nuclear relaxation rate has a strong and periodic dependence on ω, with the period determined by the PSC of the particular excitation protocol: $2\pi/T_R$ for the single pulse train and $2\pi/T_D$ for the double pulse train (Fig. 2A). The huge difference in the nuclear flip rate explains why $\omega_{N,x}$ in each QD tends to reach the value allowing the electron spin to fulfill the PSC. In QDs with the electron spin not matching the PSC, the nuclear contribution to ω changes randomly because of the light stimulated nuclear flip-flop processes on a seconds time scale. The typical range $\Delta\omega_{N,x}$ of this contribution to ω is limited by statistical fluctuation of the nuclear spin polarization. For the studied (In,Ga)As QDs, $\Delta\omega_{N,x}$ is on a GHz scale (SOM text) and comparable with the separation between the phase-synchronized modes $2\pi/T_R \sim 0.48$ GHz. As a result, the nuclear contribution occasionally drives an electron to a PSC mode, where its precession frequency is virtually frozen on a minutes time scale. This leads to the frequency focusing in each QD and to accumulation of the QDs, for which electron spins match the PSC.

The frequency focusing modifies the spin precession mode density in the QD ensemble (Fig. 2B and its closeup in C). Without focusing, the density of the electron spin precession modes is Gaussian with a width

$$\Delta\omega = \sqrt{[\Delta\omega_{N,x}]^2 + [\mu_B \Delta g_e B/(\hbar)]^2}$$, where Δg_e

is the g factor dispersion. Frequency focusing modifies the original continuum density to a comb-like distribution. Eventually the whole QD ensemble participates in a coherent precession locked on only a few precession frequencies. This suggests that a laser protocol (defined by a pulse sequence, width, and rate) can be designed to focus the electron-spin precession frequencies in the QD ensemble to a single mode. To calculate the spin precession mode density in Fig. 2, we have applied a "box model" (*29*), in which the electron wave function has a finite amplitude $1/\sqrt{V}$ inside the QD volume, V, and is zero outside (SOM text).

The quantitative appearance of the spin precession mode density depends strongly on the excitation protocol. The complex evolution of the mode density caused by the switching between pumping protocols is described by Eq. 16 in (SOM text). Some of its features observed in the FR signal can be explained qualitatively. For example, the almost instantaneous FR signal rise when switching from the single to the two pump pulse protocol in Fig. 1D can be traced to the 1/7 fraction of QDs that, after exposure to the single pump pulse protocol, already fulfill the PSC for the two pump pulse protocol without any nuclear rearrangement (Fig. 2B). In the opposite case of switching from two to single pump pulse excitation, almost all QDs, which satisfy the PSC before the switch, continue to be mode-locked afterward (Fig. 2C). Changes of nuclear spin polarization are suppressed in these QDs, leading to a dynamics in the minutes time range (SOM text) and explaining the slow FR signal decrease in Fig. 1C.

The focusing of electrons into PSC modes is directly manifested by the FR signals in Fig. 1A, because it causes comparable FR amplitudes before and after the pump pulses. The calculations demonstrate that, without frequency focusing, the FR amplitude at negative delays, A_{neg}, does not exceed 30% of the positive delay signal amplitude, A_{pos} (Fig. 3A). The strong optical pump pulses in the experiment address all QDs, and their total contribution should make the FR signal much stronger after the pulse than before, when only the mode-locked electrons are relevant. However, the nuclear adjustment increases the negative delay signal to more than 90% (Fig. 3B). This is in agreement with the experimental data in Fig. 3C, which show only the electron contribution to the FR signal. The large value of A_{neg}/A_{pos} confirms that in our experiment almost all electrons in the optically excited QD ensemble become involved in the coherent spin precession. The calculations of the intensity dependence of the ratio A_{neg}/A_{pos} show that the nuclear focusing increases the ratio of electrons involved in the coherent spin precession to their total number, n_{psc}/n, almost to unity, even at low excitation intensity (Fig. 3, D and E).

We have shown that the nuclei in singly charged QDs exposed to a periodic pulsed excitation focus almost all the electrons in the ensemble into a coherent electron spin precession. The exciting laser acts as a metronome and establishes a robust macroscopic quantum bit, which exists in dephasing free subspaces. This may open promising perspectives on the use of an ensemble of charged QDs with the single electron coherence time T_2.

References and Notes

1. S. A. Wolf *et al.*, *Science* **294**, 1488 (2001).
2. D. Loss, D. P. DiVincenzo, *Phys. Rev. A* **57**, 120 (1998).
3. I. A. Merkulov, Al. L. Efros, M. Rosen, *Phys. Rev. B* **65**, 205309 (2002).
4. A. V. Khaetskii, D. Loss, L. Glazman, *Phys. Rev. Lett.* **88**, 186802 (2002).
5. A. C. Johnson *et al.*, *Nature* **435**, 925 (2005).
6. F. H. L. Koppens *et al.*, *Science* **309**, 1346 (2005); published online 21 July 2005 (10.1126/science.1113719).
7. J. R. Petta *et al.*, *Science* **309**, 2180 (2005); published online 1 September 2005 (10.1126/science.1116955).
8. W. A. Coish, D. Loss, *Phys. Rev. B* **72**, 125337 (2005).
9. W. Yao, R.-B. Liu, L. J. Sham, *Phys. Rev. Lett.* **98**, 077602 (2007).
10. W. M. Witzel, S. Das Sarma, *Phys. Rev. Lett.* **98**, 077601 (2007).
11. A. G. Kofman, G. Kurizki, *Phys. Rev. Lett.* **93**, 130406 (2004).
12. G. Burkard, D. Loss, D. P. DiVincenzo, *Phys. Rev. B* **59**, 2070 (1999).
13. W. A. Coish, D. Loss, *Phys. Rev. B* **70**, 195340 (2004).
14. D. Gammon *et al.*, *Science* **277**, 85 (1997).
15. J. M. Taylor, C. M. Marcus, M. D. Lukin, *Phys. Rev. Lett.* **90**, 206803 (2003).
16. A. Imamoglu, E. Knill, L. Tian, P. Zoller, *Phys. Rev. Lett.* **91**, 017402 (2003).
17. J. M. Kikkawa, D. D. Awschalom, *Science* **287**, 473 (2000).
18. M. N. Leuenberger, D. Loss, M. Poggio, D. D. Awschalom, *Phys. Rev. Lett.* **89**, 207601 (2002).
19. A. Greilich *et al.*, *Science* **313**, 341 (2006).
20. A. Greilich *et al.*, *Phys. Rev. Lett.* **96**, 227401 (2006).
21. Materials and methods are available on *Science* Online.
22. J. M. Kikkawa, D. D. Awschalom, *Phys. Rev. Lett.* **80**, 4313 (1998).
23. A. Greilich *et al.*, *Phys. Rev. B* **75**, 233301 (2007).
24. D. Paget, *Phys. Rev. B* **25**, 4444 (1982).
25. V. L. Berkovits, A. I. Ekimov, V. I. Safarov, *Sov. Phys. JETP* **38**, 169 (1974).
26. M. I. Dyakonov, V. I. Perel, in *Optical Orientation*, F. Meier, B. P. Zakharchenja, Eds. (North-Holland, Amsterdam, 1984).
27. M. Kroutvar *et al.*, *Nature* **432**, 81 (2004).
28. A. Khaetskii, Yu. V. Nazarov, *Phys. Rev. B* **61**, 12639 (2000).
29. S. M. Ryabchenko, Yu. G. Semenov, *Sov. Phys. JETP* **84**, 1412 (1983).
30. M. I. Dyakonov, V. I. Perel, *Sov. Phys. JETP* **65**, 362 (1973).
31. A. Abragam, *The Principles of Nuclear Magnetism* (Oxford Univ. Press, London, 1961), p. 273.

32. We are grateful to S. Erwin, T. Kennedy, and I. A. Merkulov for their critical suggestions on the manuscript. This work was supported by the Bundesministerium für Bildung and Forschung program "nanoquit," the Defence Advance Research Project Agency Quantum Information Science and Technology program, the Office of Naval Research, and the Deutsche Forschungsgemeinschaft (Forschergruppe "Quantum Optics in Semiconductor Nanostructures").

Supporting Online Material

www.sciencemag.org/cgi/content/full/317/5846/1896/DC1
Materials and Methods
SOM Text
References

21 June 2007; accepted 29 August 2007
10.1126/science.1146850